coatings

MDPI

Article

Anti-Corrosive Properties of an Effective Guar Gum Grafted 2-Acrylamido-2-Methylpropanesulfonic Acid (GG-AMPS) Coating on Copper in a 3.5% NaCl Solution

Ambrish Singh [1,2,*], Mingxing Liu [1,2], Ekemini Ituen [1,2] and Yuanhua Lin [1,2,*]

[1] School of Materials Science and Engineering, Southwest Petroleum University, Chengdu 610500, China; m1763902986@163.com (M.L.); ebituen@gmail.com (E.I.)

[2] State Key Laboratory of Oil and Gas Reservoir Geology and Exploitation, Southwest Petroleum University, Chengdu 610500, China

* Correspondence: vishisingh4uall@gmail.com (A.S.); yhlin28@163.com (Y.L.); Tel.:+028-83037401 (Y.L.)

Received: 23 December 2019; Accepted: 24 February 2020; Published: 5 March 2020

Abstract: Guar gum grafted 2-acrylamido-2-methylpropanesulfonic acid (GG-AMPS) was synthesized using guar gum and AMPS as the base ingredients. The corrosion inhibition of copper was studied using weight loss, electrochemical, and surface characterization methods in a 3.5% sodium chloride (NaCl) solution. Studies including weight loss were done at different acid concentrations, different inhibitor concentrations, different temperatures, and different immersion times. The weight loss studies showed the good performance of GG-AMPS at a 600 mg/L concentration. This concentration was further used as the optimum concentration for all of the studies. The efficiency decreased with the rise in temperature and at higher concentrations of acidic media. However, the efficiency of the inhibition increased with the additional immersion time. Electrochemical methods including impedance and polarization were employed to calculate the inhibition efficiency. Both of the techniques exhibited a good inhibition by GG-APMS at a 600 mg/L concentration. Surface studies were conducted using scanning electrochemical microscopy (SECM), scanning electron microscopy (SEM), and atomic force microscopy (AFM) methods. The surface studies showed smooth surfaces in the presence of GG-AMPS and rough surfaces in its absence. The adsorption type of GG-AMPS on the surface of the copper followed the Langmuir adsorption model.

Keywords: corrosion; guar gum; coatings; electrochemical impedance spectroscopy (EIS); SECM; AFM

1. Introduction

Copper is used worldwide because of its good conductivity, availability, and large tenders. Almost all companies use copper in one way or another, because of its varied applications. Copper is an appropriate material for electrodes, wires, joints, and couplings [1]. An NaCl solution can cause severe corrosion in metals and alloys [2]. It can cause pitting corrosion under the coatings by forming blisters. These pits are difficult to detect under the coatings, and can cause fatal accidents and a shutdown of the systems. Known also as rock salt or common salt, sodium chloride is abundantly found in nature and mostly in sea water. Marine corrosion is very common and causes billions of dollars of losses globally. So, there is always a need to find solutions to marine corrosion.

The application of corrosion inhibitors is currently the most cost-efficient means of dealing with copper corrosion [3]. The corrosion inhibitors used at this stage are mainly organic corrosion inhibitors, because organic molecules may contain O, N, and S, as well as other atoms with unshared

pair electrons and π-bonds [3]. Such organic molecules can be empty orbitals, which interact with copper surfaces [3]. The d-orbital acts to form a protective film to achieve corrosion protection. Glue extracted from natural plants is one of them. Gum contains a large amount of O atoms, and has received a lot of attention and has been widely studied. At the same time, the use of gums as corrosion inhibitors can effectively improve the utilization rate of natural plants. Chemical compounds or inhibitors are used to mitigate corrosion as one of the common available methods. These compounds are inorganic and organic in nature. They are rich in carbon, oxygen, nitrogen, sulfur, benzene rings, and double bonds in their molecular structures [4]. In the recent decade, the corrosion fraternity has been concerned with finding green and environment-friendly inhibitors [5]. Plant extracts, as potential corrosion inhibitors, have been used by several authors [6–10]. The shortcoming of using plant extracts is that they tend to develop fungi/bacteria on their surfaces after some time, and this affects their inhibition efficiency. So, the search for green polymers or biopolymers has been sought worldwide. Several polymers have been studied with heteroatoms in their structures [11–15]. The multifunctional groups in the polymers can easily adsorb or attach to any metal surface, thereby protecting them from corrosion. Polymers may prove to be better than the low molecular inhibitors used in the acidization process. Biocompatible compounds have also been used as inhibitors because of their cost effectiveness, ease of availability, and low-cost machines used. Our motivation was to develop a compound with all of the qualities of a polymer, in addition to being non-toxic and environmentally benign. Thus, guar gum grafted 2-acrylamido-2-methylpropanesulfonic acid (GG-AMPS) was synthesized as a green compound to cope with environmental regulations, and to be used effectively in high concentrations.

A survey of the literature reveals that no work has been done using GG-AMPS as a corrosion inhibitor in an NaCl solution. GG-AMPS has a nitrogen atom, oxygen atom, and sulfur atom in its molecular structure, which provide a good adsorption approach, leading to good bonding and complex grouping on the metal surface. The presence of hydroxyl groups at different points makes it a potential inhibitor that can share electrons and take part in good bond formation. This paper elucidates the inhibition effect of GG-AMPS for copper in a 3.5% NaCl media. The mitigation properties of GG-AMPS were conducted using static weight-loss methods and electrochemical methods. In the meantime, the surfaces of copper were examined by scanning electrochemical microscopy (SECM), scanning electron microscopy (SEM), and atomic force microscopy (AFM).

2. Experimental

2.1. Copper Samples

In all of the experiments, such as for the weight loss, the electrochemical and surface morphology of the pure copper samples were utilized. Each of the samples employed for weight loss were cut into rectangle coupons. Prior to the experiments, the surfaces were abraded with silicon sheets of grades 300 to 1200, cleaned with acetone and distilled water, and vacuum-dried. The dimensions of the copper samples employed for the weight loss tests were 2.0 cm × 2.5 cm × 0.2 cm.

2.2. Corrosive Medium

The inhibitor coatings were concentrated in the range of 100 to 600 mg/L for all of the studies. A 3.5% sodium chloride solution was used as the corrosive medium. It was prepared using pure NaCl and double-distilled water. A freshly prepared solution was used for each of the experiments. The different concentrations of inhibitor solutions were prepared by adding a calculated amount of inhibitor into the corrosive medium.

2.3. Synthesis of GG-AMPS

The synthesis of GG-AMPS was conducted according to the previous reference [16–18]. One gram of guar gum was slowly dissolved in 100 mL of distilled water. Then, 0.2 g of potassium persulfate was added to the guar gum solution, and the reaction continued for 1 h in a water bath at

70 °C. After that, 2 g of 2-acrylamide-2-methyl-1-propane sulfonic acid (AMPS) and 0.2 g of N, N′-methylenebisacrylamide were added to the above solution, and the reaction continued for 3 h at the same temperature (70 °C). The whole reaction process was carried out in a nitrogen atmosphere. After the solution was cooled, the excess acetone was added to the solution so as to separate the desired product. The precipitates were filtered and dried in vacuum at 50 °C for 24 h to a constant weight. The product was guar gum grafted with 2-acrylamide-2-methyl-1-propane sulfonic acid (GG-AMPS). The compound obtained was further characterized by infrared (IR) spectroscopy. The plan of the synthesis and molecular structure of the inhibitor coating is shown in Figure 1.

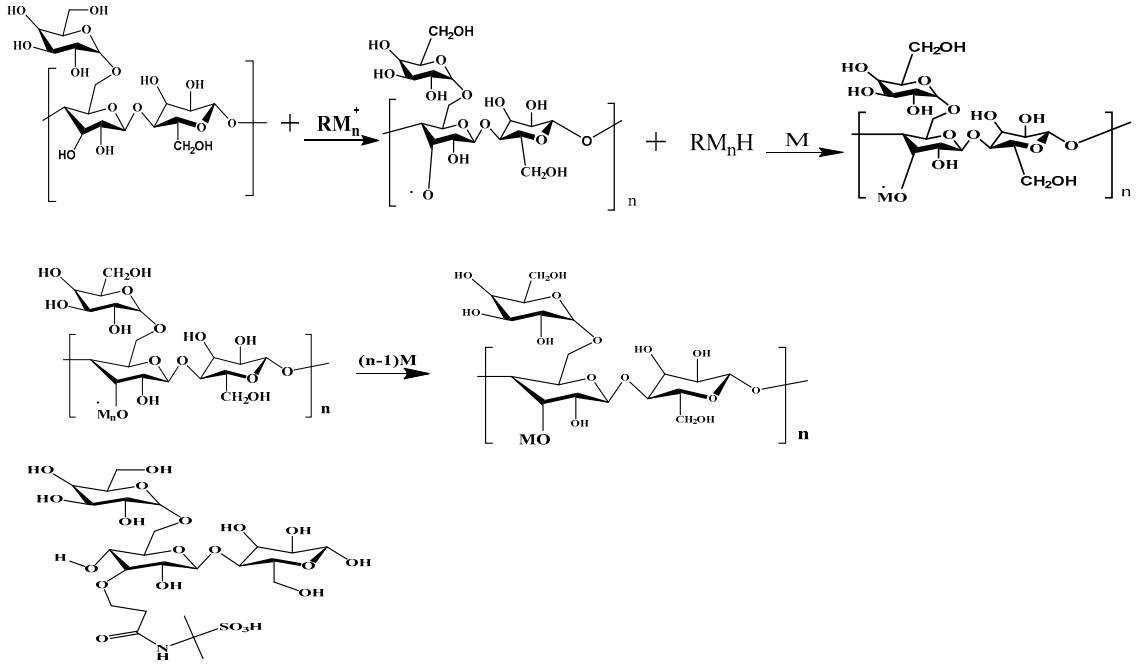

Figure 1. Molecular structure and synthesis scheme of guar gum grafted 2-acrylamido-2-methylpropanesulfonic (GG-AMPS). M = AMPS.

2.4. Infrared Spectroscopy

IR spectroscopy was conducted using the Nicolette 6700 infrared spectrometer of Thermo Electric Company Inc. from the USA (West Chester, PA). The infrared spectrum of the GG-AMPS is shown in Figure 2.

Figure 2 shows the IR spectrum of the guar gum and GG-AMPS. In Figure 2, 3461 cm^{-1} indicates the tensile vibration of O–H in the guar gum. In addition, the weak peak near 2926 cm^{-1} is the C–H, and the peak at 1638 cm^{-1} is the vibration peak of the six-membered rings. In Figure 2, the small peaks at 1552 and 1300 cm^{-1} are the bending vibrations of N–H in the AMPS amide group, and the wide peak at 3408 cm^{-1} is the overlap of the N–H stretching band and O–H stretching band, which resulted in a certain movement of the wide peak at 3461 cm^{-1} in the guar gum. The peak at 1657 cm^{-1} and its adjacent peak are the result of the overlapping of the C=O vibration and –CONH– vibration in –CO_2H. The peaks at 1375 and 1458 cm^{-1} are the C–H bending vibrations in –CH_3, –CH_2, and –CH. The peaks at 1220 and 1042 cm^{-1} are characteristic peaks of a sulfonic group. Figure 2 reveals that AMPS was successfully grafted with guar gum.

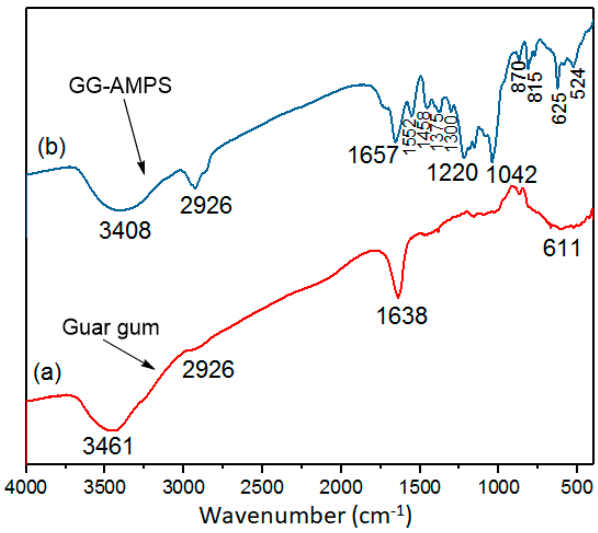

Figure 2. IR spectrum of GG-AMPS.

2.5. Weight Loss

The duration of all of the weight loss tests was determined following the ASTM G31-2004 standard [19]. The duration of the experiments selected for all of the tests was 24 h. The copper coupons were cleaned with water and then rinsed with Clarke's solution for 5 min. The coupons were then exposed to vacuum drying. The obtained weight loss values were used to calculate the corrosion rate of the metal in the corrosive media. Each of the tests were performed in triplicate and the mean values were reported. The corrosion rates were calculated using the following equation:

$$C_R(mm/y) = \frac{87.6W}{atD} \quad (1)$$

where W is the average weight loss of copper specimens (mg), a is total area of copper specimen, t is the immersion time (h), and D is the density of copper in (g·cm^{-3}).

2.6. Electrochemical Analysis

A Gamry potentiostat workstation (Gamry, Warminster, PA, USA) was utilized for the electrochemical tests. The potentiostat was connected to a cell assembly, which consisted of a reference electrode, counter electrode, and working electrode. Prior to the start of the experiments, the working electrode (copper) was exposed to the 3.5% NaCl solution for 30 min, so as to keep the potential (E_{corr}) stable.

The range of the frequency selected was from 100 kHz to 10 mHz, at an amplitude of 10 mV per decade for all of the electrochemical impedance tests. The evaluation of the inhibition efficiency was done using the following equation:

$$\eta\% = \left(1 - \frac{R_{ct}}{R_{ct(i)}}\right) \times 100 \quad (2)$$

where R_{ct} and $R_{ct(i)}$ are the charge transfer resistances without and with GG-AMPS, respectively.

The potentiodynamic polarization tests were conducted in the limit of −250 to 250 mV, with a 0.167 mV/s scan rate. The following equation was used to determine the efficiency of the coating:

$$\eta\% = \left(1 - \frac{i_{corr(i)}}{i_{corr}}\right) \times 100 \quad (3)$$

where i_{corr} and $i_{corr(i)}$ are the corrosion current densities without and with GG-AMPS, respectively.

2.7. Scanning Electrochemical Microscopy (SECM)

The SECM tests were performed using a Princeton workstation equipped with Versa scan software (3000, Versa, TX, USA). The microprobe was made of a silver (Ag)/Pt wire inside a glass tube with a diameter of 10 μm. The probe vibrated over the metal surface at an average distance of 100 μm, and the scanned area was 20 μm × 20 μm.

2.8. Scanning Electron Microscopy (SEM)

The scanning electron microscopy (SEM) was done to detect the changes in the external area of the metal. The SEM was conducted using a Tescan machine (S800, Tescan, Shanghai, China) equipped with a Zeiss lens (Zeiss, Shanghai, China). The samples were washed with a sodium bicarbonate solution in order to remove the corrosion products, followed by distilled water prior to surface exposure.

2.9. Atomic Force Microscopy (AFM)

The AFM experiments were conducted using a Dimension Icon Brock instrument (HPI, Bruker, Karlsruhe), made in Germany, for all of the copper coupons. Once the tests were completed, the images obtained were sent to Nanoscope analysis software (2.0), version v1.40r1, so as to obtain the 3D figures. The average roughness and the peak roughness were further confirmed using the linear fitting of the 2D figures.

3. Results and Discussion

3.1. Weight Loss Experiment

3.1.1. Effect of Concentration, Time, and Temperature

The effect of the GG-AMPS concentrations on the protective covering of the copper surfaces is portrayed in the form of a concentration vs. inhibition efficiency graph (Figure 3a). From the figure, it is evident that the mitigation activity of GG-AMPS rose with the increase in concentration, and attained values of 95% at 600 mg/L. This increase in mitigation ability was due to the adsorption of the GG-AMPS molecules onto the wide area of the copper surface. Figure 3b displays the increase in inhibition efficiency with immersion time, for up to 12 h. This discovery points to the molecular structure of GG-AMPS having a big effect on the values of inhibition efficiency. Figure 3c depicts the influence of temperature on the inhibition efficiency of GG-AMPS. The efficiency was found to decrease with an increase in temperature. This may have been the result of the desorption of the coating from the copper surface. So, for this coating to be used at high temperatures, the concentration of the coating should be increased. Figure 3d displays the influence of the inhibition efficiency with the NaCl concentration. The efficiency was seen to decrease with the increase in NaCl concentration. This may be due to the NaCl solution penetrating the coating on the copper surface, causing pitting corrosion. In this study, the inhibitor molecules had π-electrons in the benzene ring and non-bonding electrons on the heteroatoms, such as oxygen, sulfur, and nitrogen, which assist the molecules in their adsorption onto the copper surface [20].

The adsorption of the coating on any metal surface also depends on the number of electron-donating functional groups attached to the structure. A greater number of electron-donating groups can help with better adsorption and bond formation, which can lead to a better mitigation of corrosion. GG-AMPS consists of OH, SO_3H, and NH groups, which may be a reason for its good mitigation abilities in the corrosion of copper in sodium chloride media.

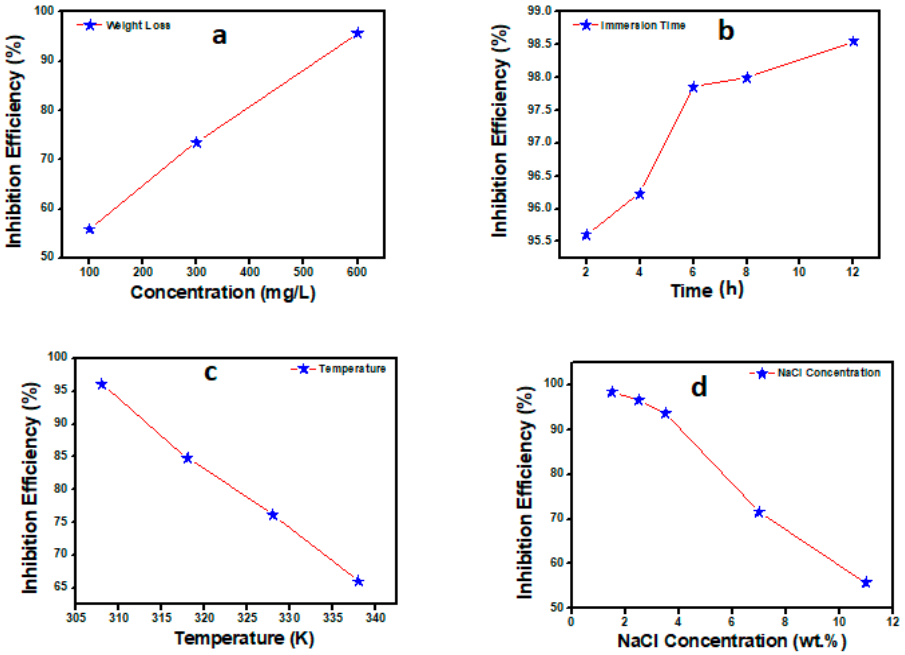

Figure 3. (**a**) Variation of inhibition efficiency (%) with inhibitor concentration. (**b**) Variation of inhibition efficiency (%) with immersion time. (**c**) Variation of inhibition efficiency (%) with temperature. (**d**) Variation of inhibition efficiency (%) with NaCl concentration.

3.1.2. Adsorption Isotherm of Inhibitor on Copper

The adsorption of molecules on the metal surface can be better explained using Langmuir, Frumkin, Flory Huggins, and Temkin isotherms. The obtained experimental data can be fit using the equations of these isotherms. The best fit gives a linear slope with regression coefficient values approaching unity. The fitted experimental values showed that Langmuir was the best out of all of the equations (Figure 4). The following equation was used to determine the fitted results of the isotherm [21]:

$$\frac{C_{\text{inh}}}{\theta} = \frac{1}{K_{\text{ads}}} + C_{\text{inh}} \quad (4)$$

where C_{inh} is the GG-AMPS concentration (mg/L), and θ and K_{ads} represent the surface coverage and adsorption constant, respectively.

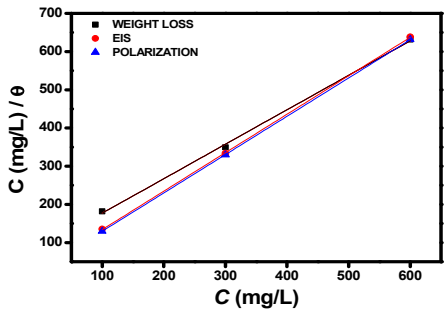

Figure 4. Langmuir adsorption isotherm plots using the values of weight loss, electrochemical impedance spectroscopy (EIS), and polarization.

3.2. Electrochemical Tests

3.2.1. Electrochemical Impedance Spectroscopy (EIS) Studies

The behavior of the copper electrode was investigated by electrochemical impedance tests. The impedance nature of the metal is represented in the form of Nyquist graphs (Figure 5a). As reported in Figure 5a, at a higher frequency, a capacitive loop is seen, which contains a straight line, tending to be a semicircle. The semicircle is normally the result of the capacitance of double-layer and charge-transfer resistance [22]. The presence of two time constants can be seen in the Nyquist and bode figures. The presence of two time constants may have been because of the roughness and inhomogeneity of the metal surface after corrosion. In addition, the diameter capacitance with GG-AMPS was bigger in comparison with the blank. Meanwhile, the diameter got bigger with higher concentrations of GG-AMPS. This was because the GG-AMPS molecules that were adsorbed on the copper surface formed a barrier and enhanced the corrosion resistance properties [23–25].

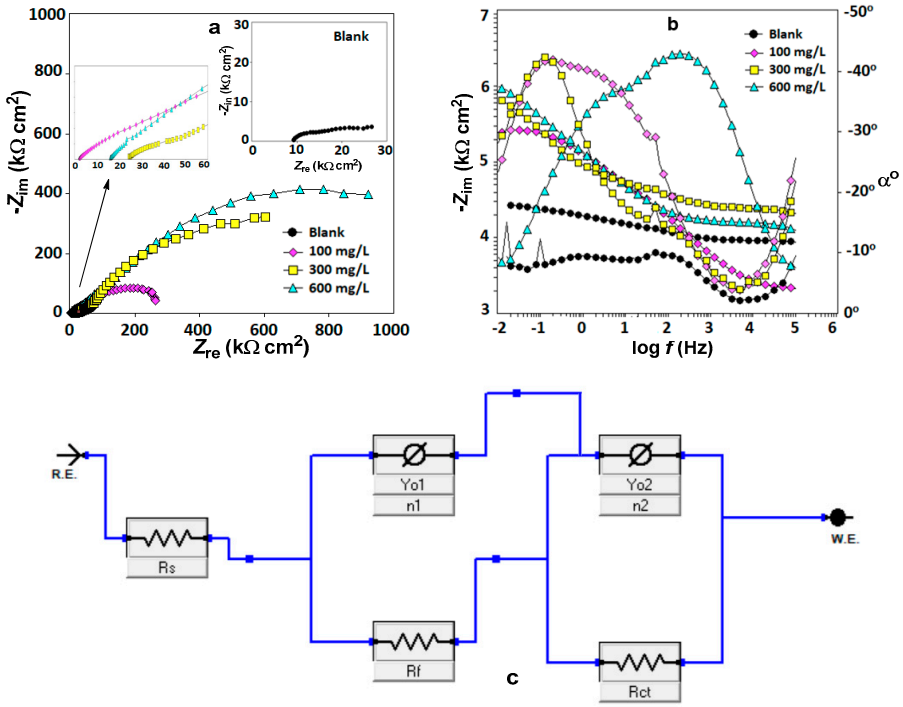

Figure 5. (**a**) Nyquist plots at different concentrations of GG-AMPS. (**b**) Bode, phase-angle plots at different concentrations of GG-AMPS. (**c**) Equivalent circuit used to fit and analyze the data.

In the bode plots (Figure 5b), the slope values tended to increase in the presence of GG-AMPS, rather than in its absence. This indicates the inhibition action of GG-AMPS on the copper surfaces. In the phase angle plots (Figure 5b), at the intermediate frequency, the pinnacle of the phase angle increased as the GG-AMPS concentration increased. The highest peak was observed at 43.2° for copper at a 600 mg/L inhibitor concentration. This was due to the corrosion mitigation on the copper surfaces by the GG-AMPS protective shield, which that isolated the copper from the corrosive media [26]. The binding of the GG-AMPS molecules with the metal surface was quite strong and stable, which finally enhanced its corrosion resistance quality. For the impedance data calculation, the circuit used is shown in Figure 5c. The circuit used was drawn using the model editor in Echem analyst. It contained charge-transfer resistance (R_{ct}), a solution resistor (R_s), film resistance (R_f), and two constant phase elements (CPEs). The CPEs were included in the circuit for the perfect fitting of the Nyquist curves, as they balance the deviation of surface roughness, disruption, imperfectness, impurity, and adsorption [27–30].

The CPE impedance is given below:

$$Z_{\mathrm{CPE}} = Y_{\mathrm{o}}^{-1}(i\omega)^{-n} \quad (5)$$

where Y_0, ω, i, and n are the constant, angular frequency, an imaginary number, and an empirical exponent, respectively.

Table 1 shows the impedance values of the fitted curves. It can be seen that the R_{ct} and Y_0 parameters at all of the concentrations of GG-AMPS display a reverse pattern. This process is credited to the GG-AMPS molecules adsorbing onto the copper surface, which finally enhances the copper corrosion resistance attributes [31]. The value of R_{ct} at 600 mg/L for GG-AMPS is 905 kΩ·cm^2. Thus, GG-AMPS provides a good resistance to corrosive solutions. The rise in n values with the increase in GG-AMPS concentration was due to their adsorption and finally enhancement of their homogeneity [32]. Thus, with a decent number of heteroatom functional groups, the corrosion inhibition property increased.

Table 1. Electrochemical impedance parameters in the absence and presence of different concentrations of GG-AMPS at 308 K.

C_{inh}	R_s	R_{ct}	n_1	Y_{o1}	n_2	Y_{o2}	R_f	X^2	η_{EIS}
(mg/L)	(kΩ·cm^2)	(kΩ·cm^2)		(μF/cm^2)		(μF/cm^2)	(kΩ·cm^2)	×10^{-3}	(%)
Blank	9.29	87	0.72	57.8	0.37	59.2	7.2	1.01	–
100	3.01	130	0.76	34.2	0.43	51.1	20.4	3.50	33.0
300	23.5	568	0.81	23.5	0.59	45.4	310.2	4.53	84.6
600	15.51	905	0.83	19.5	0.74	31.3	415.5	2.73	90.3

X^2 refers to Chi square.

3.2.2. Potentiodynamic Polarization Tests

The polarization plots of copper in NaCl solutions without and with different concentrations of GG-AMPS are represented in Figure 6. Several essential electrochemical factors, like the corrosion current density (i_{corr}), corrosion potential (E_{corr}), cathodic Tafel slope (β_c), anodic Tafel slope (β_c), and inhibition efficiency (η%), are tabulated in Table 2. The analysis of Table 2 suggests that the corrosion current density shifted from 98.7 μA/cm^2 (3.5% NaCl) to 4.9 μA/cm^2 (600 mg/L GG-AMPS), and this represents that the GG-AMPS coating was effective for the mitigation of corrosion. The value of maximal efficiency as obtained was 95% at 600 mg/L. As can be seen, after the inclusion of GG-AMPS in the corrosive media, both the anodic and cathodic current density were reduced. The addition of GG-AMPS in higher concentrations caused more H^+ ion reduction in the system than the anodic dissolution process. As is evident in Figure 6, the collateral cathodic slopes suggest the conversion of H^+ to H_2 was not varied. Similarly, with higher concentrations of GG-AMPS, the β_c values were shifted, suggesting that GG-AMPS affected the kinetics of H_2 evolution. This may be accredited to the diffusion or the shield phenomenon [33]. Likewise, the values of β_a also underwent a modification with the increase in the GG-AMPS concentration, suggesting that the designed coating primarily underwent adsorption all over the copper surface. This phenomenon shows the mitigation of the corrosion reaction by obstructing the activated centers, without modifying the mechanism of the anodic process [34].

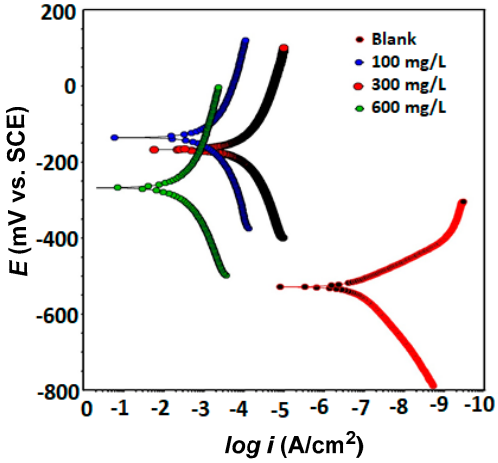

Figure 6. Potentiodynamic polarization curves in the absence and presence of different concentrations of GG-AMPS.

Table 2. Electrochemical polarization parameters in the absence and presence of different concentrations of GG-AMPS at 308 K.

Inhibitor	E_{corr}	i_{corr}	β_a	$-\beta_c$	η
(mg/L)	(mV/SCE)	(μA/cm²)	(mV/dec)	(mV/dec)	(%)
Blank	−579	98.7	67	358	–
100	−145	21.2	267	79	78.5
300	−189	12.0	233	73	87.8
600	−293	4.9	199	84	95.0

In addition, the polarization curves showed that the addition of GG-AMPS mitigated both the cathodic and anodic processes. Therefore, the coating can be categorized into mixed forms. Nevertheless, the variations in the E_{corr} values in the presence of the coating were towards the anodic route, as compared with those without the coating, indicating that GG-AMPS is predominantly cathodic.

3.3. Scanning Electrochemical Microscopy (SECM)

Scanning electrochemical microscopy is very useful for detecting localized corrosion on the metal surface. Figure 7a,b shows the 2D and 3D pictures of the *x*-axis for copper without GG-AMPS in a seawater solution. A very high current was observed in the 2D maps and 3D structures (Figure 7a,b). This can be endorsed by the straight connection of the probe with the copper surface. As the probe was moved at a certain visible corroded part on the metal surface observed through the camera, the corrosion profile was detected. However, for the copper surface with the GG-AMPS film on it, the 2D and 3D maps showed a lower current (Figure 7c,d). A lower current was observed in the presence of the GG-AMPS film, which may have been due to the GG-AMPS coating on the copper surface forming a hydrophobic film that repelled the corrosive solution. This phenomenon indicated that the GG-AMPS film protected the copper surface well from corrosion in the NaCl solution.

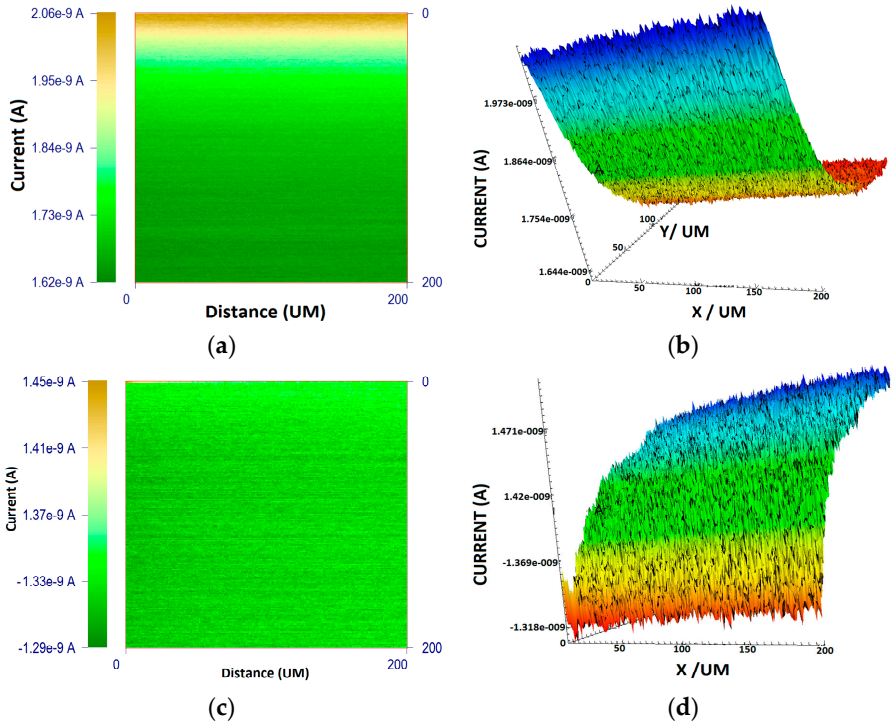

Figure 7. Scanning Electrochemical Microscopy (SECM) images of (**a**) 2D and (**b**) 3D copper surface in 3.5% NaCl solution and (**c**) 2D and (**d**) 3D copper surface coated with GG-AMPS in 3.5% NaCl solution.

3.4. Scanning Electron Microscopy (SEM)

The copper coupons with 600 mg/L GG-AMPS and 3.5% NaCl were exposed to SEM, as depicted in Figure 8. The surface morphology of the copper without GG-AMPS was very rough with several corrosion products, because of the rampant dissolution and deterioration of the metal (Figure 8a). Nevertheless, the addition of the GG-AMPS showed a smooth copper surface (Figure 8a). However, the surface showed a porous coating with abraded lines visible through them. This phenomenon suggested that, with GG-AMPS, the rate of corrosion was decreased due to the GG-AMPS coating having formed a conserving film over the copper surface.

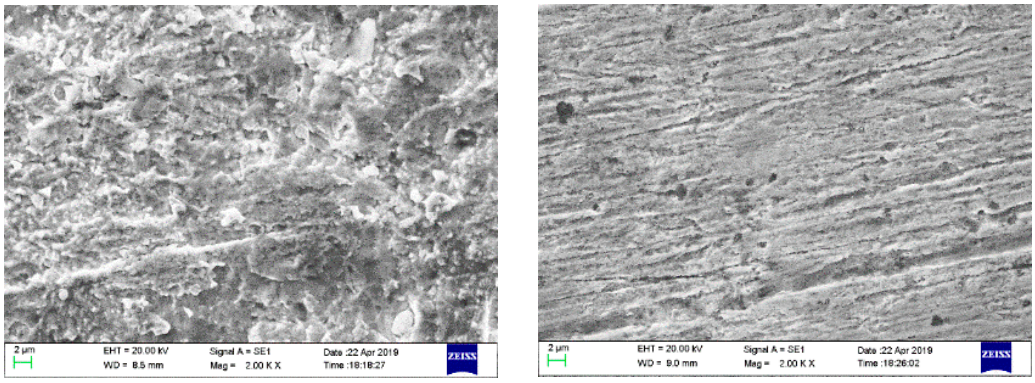

Figure 8. SEM images of a (**a**) copper surface in a 3.5% NaCl solution, and a (**b**) copper surface coated with GG-AMPS in a 3.5% NaCl solution.

3.5. Atomic Force Microscope (AFM)

The 3D micro-structural pictures of the copper surface are displayed in Figure 9. The clear indication of the terrible deterioration of the copper surface without coating due to corrosion can be seen in Figure 9a,b. Nevertheless, the roughness of the copper surface was comparatively decreased with the addition of GG-AMPS (Figure 9c,d). This anti-corrosive nature of the coating is surely because of the good binding with the metal surface.

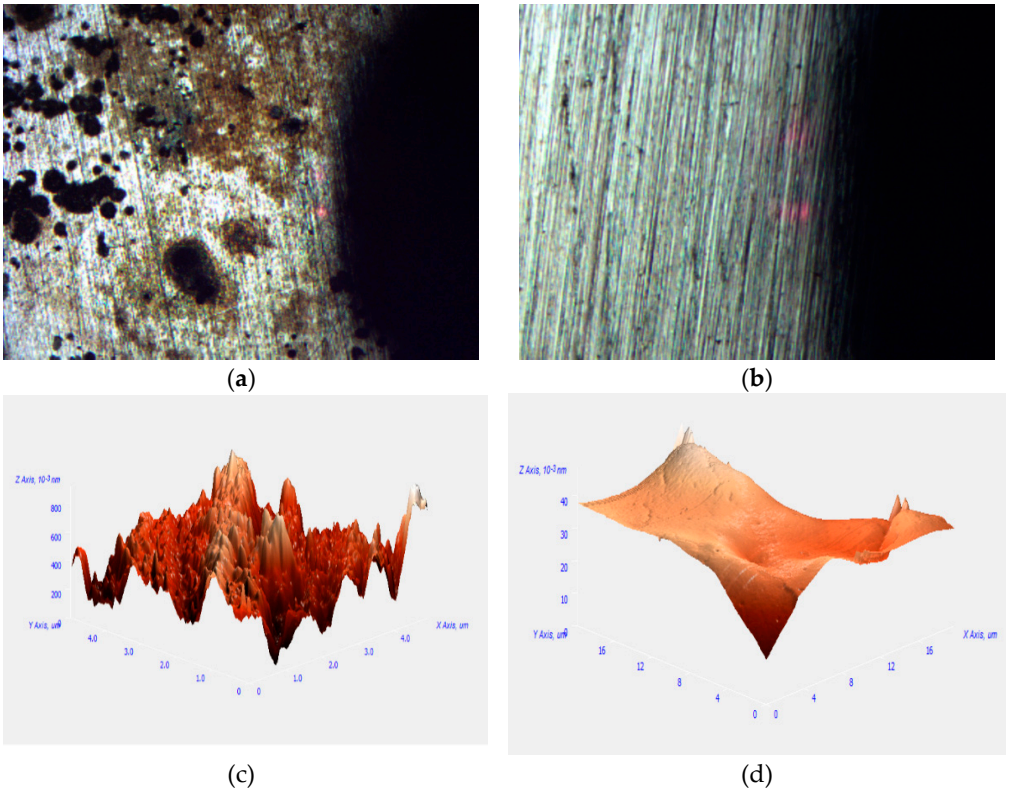

Figure 9. Optical image (**a**) copper surface in a 3.5% NaCl solution (**b**) copper surface coated with GG-AMPS in a 3.5% NaCl solution; AFM images (**c**) copper surface in a 3.5% NaCl solution (**d**) copper surface coated with GG-AMPS in a 3.5% NaCl solution.

4. Conclusions

The tested GG-AMPS coating is good for copper in a 3.5% NaCl solution. The experimental investigations suggest that the number of heteroatoms present in the GG-AMPS coating helps with the good binding to the copper surfaces, thereby reducing the corrosion rate. The SECM suggests that the inductive effect is because of the GG-AMPS coating. SEM and AFM suggest the potential corrosion mitigation of GG-AMPS coatings on copper surfaces in a 3.5% NaCl solution.

Author Contributions: Conceptualization, A.S. and M.L.; methodology, M.L. and E.I.; software, A.S.; validation, A.S. and Y.L.; formal analysis and investigation, A.S. and M.L.; resources, data curation and writing—original draft preparation, Y.L., A.S., M.L. and E.I.; writing—review and editing, visualization and supervision, A.S.; project administration and funding acquisition, A.S., Y.L. and E.I. All authors have read and agreed to the published version of the manuscript.

Funding: The authors are thankful to the Sichuan 1000 Talent Fund; the financial assistance provided by the Youth Scientific and Innovation Research Team for Advanced Surface Functional Materials, Southwest Petroleum University (No. 2018CXTD06); and the open fund project (No. X151517KCL42).

Acknowledgments: Authors would like to acknowledge the help provided by Mumtaz Ahmad Quraishi and Kashif Rahmani Ansari, KFUPM, Saudi Arabia. Authors also extend gratitude to Xu Xihua for her help in the experimental procedures.

Conflicts of Interest: The authors declare no conflict of interest.

References

1. Singh, A.; Ituen, E.; Ansari, K.R.; Chauhan, D.S.; Quraishi, M.A. Surface protection of X80 steel by Epimedium extract and its iodide-modified composites in simulated acid wash solution: A greener approach for corrosion inhibition. *New J. Chem.* **2019**, *43*, 8527–8538.
2. Du, P.; Li, J.; Zhao, Y.; Dai, Y.; Yang, Z.; Tian, Y. Corrosion characteristics of Al alloy/galvanized-steel Couple in NaCl solution. *Int. J. Electrochem. Sci.* **2018**, *13*, 11164–11179.
3. Antonijevic, M.M.; Petrovic, M.B. Copper corrosion inhibitors. A review. *Int. J. Electrochem. Sci.* **2008**, *3*, 1–28.
4. Ramachandran, S.; Jovancicevic, V. Molecular modeling of the inhibition of mild copper carbon dioxide corrosion by imidazolines. *Corrosion* **1999**, *55*, 259–267.
5. Ansari, K.R.; Quraishi, M.A.; Singh, A. Pyridine derivatives as corrosion inhibitors for N80 in 15% HCl: Electrochemical, surface and quantum chemical studies. *Measurement* **2015**, *76*, 136–147.
6. Sastri, V.S. Green Corrosion Inhibitors. In *Theory and Practice*, 1st ed.; John Wiley & Sons: Hoboken, NJ, USA, 2011.
7. Yang, Y.; Yin, C.; Singh, A.; Lin, Y. Electrochemical study of commercial and synthesized green corrosion inhibitors for N80 steel in acidic liquid. *New J. Chem.* **2019**, *43*, 16058–16070.
8. Fonseca, T.; Gigante, B.; Gilchrist, T.L. A short synthesis of phenanthro [2,3-d] imidazoles from dehydroabietic acid. Application of the methodology as a convenient route to benzimidazoles. *Tetrahedron* **2001**, *57*, 1793–1799.
9. Jevremovic', I.; Singer, M.; Nešic', S.; Miškovic'-Stankovic', V. Inhibition properties of self-assembled corrosion inhibitor talloil diethylenetriamine imidazoline for mild copper corrosion in chloride solution saturated with carbon dioxide. *Corros. Sci.* **2013**, *77*, 265–272.
10. Singh, A.; Ansari, K.R.; Quraishi, M.A.; Lgaz, H. Effect of electron donating functional groups on corrosion inhibition of J55 steel in sweet corrosive environment: Experimental, density functional theory and molecular dynamic simulation. *Materials* **2019**, *12*, 17, doi:10.3390/ma12010017.
11. Desimone, M.P.; Gordillo, G.; Simison, S.N. The effect of temperature and concentration on the corrosion inhibition mechanism of an amphiphilic amidoamine in CO_2 saturated solution. *Corros. Sci.* **2011**, *53*, e4033–e4043.
12. Gonzalez-Rodriguez, J.G.; Zeferino-Rodriguez, T.; Ortega, D.M.; Serna, S.; Campillo, B.; Casales, M.; Valenzuela, E.; Juarez-Islas, J. Effect of microstructure on the CO_2 corrosion inhibition by carboxy amidoimidazolines on a pipeline copper. *Int. J. Electrochem. Sci.* **2017**, *2*, 883–896.
13. He, Y.; Yang, R.; Zhou, Y.; Ma, L.; Zhang, L.; Chen, Z. Water soluble Thiosemicarbazideimidazole derivative as an efficient inhibitor protecting P110 carbon copper from CO_2 corrosion. *Anti Corros. Methods Mater.* **2016**, *63*, 437–444.
14. He, Y.; Zhou, Y.; Yang, R.; Ma, L.; Chen, Z. Imidazoline derivative with four imidazole reaction centers as an efficient corrosion inhibitor for anti-CO_2 corrosion. *Russ. J. Appl. Chem.* **2015**, *88*, 1192–1200.
15. Kandemirli, F.; Sagdinc, S. Theoretical study of corrosion inhibition of amides and thiosemicarbazones. *Corros. Sci.* **2007**, *49*, 2118–2130.
16. Biswas, A.; Das, D.; Lgaz, H.; Pal, S.; Nair, U.G. Biopolymer dextrin and poly (vinyl acetate) based graft copolymer as an efficient corrosion inhibitor for mild steel in hydrochloric acid: Electrochemical, surface morphological and theoretical studies. *J. Mol. Liq.* **2019**, *275*, 867–878.
17. Biswas, A.; Pal, S.; Udayabhanu, G. Experimental and theoretical studies of xanthan gum and its graft co-polymer as corrosion inhibitor for mild steel in 15% HCl. *Appl. Surf. Sci.* **2015**, *30*, 173–183.
18. Biswas, A.; Mourya, P.; Mondal, D.; Pal, S.; Udayabhanu, G. Grafting effect of gum acacia on mild steel corrosion in acidic medium: Gravimetric and electrochemical study. *J. Mol. Liq.* **2018**, *251*, 867–878.
19. *ASTM G31-72 Standard Practice for Laboratory Immersion Corrosion Testing of Metals*; ASTM International: West Conshohocken, PA, USA, 2004.
20. Singh, A.; Ansari, K.R.; Haque, J.; Dohare, P.; Lgaz, H.; Salghi, R.; Quraishi, M.A. Effect of electron donating functional groups on corrosion inhibition of mild steel in hydrochloric acid: Experimental and quantum chemical study. *J. Taiwan Inst. Chem. Eng.* **2018**, *82*, 470–479.
21. Singh, A.; Soni, N.; Deyuan, Y.; Kumar, A. A combined electrochemical and theoretical analysis of environmentally benign polymer for corrosion protection of N80 steel in sweet corrosive environment. *Results Phys.* **2019**, *13*, 102116.

22. Xu, X.; Singh, A.; Sun, Z.; Ansari, K.R.; Lin, Y. Electrochemical, surface and quantum chemical studies of novel imidazole derivatives as corrosion inhibitors for J55 steel in sweet corrosive environment. *R. Soc. Open Sci.* **2017**, *4*, 170933–170951.
23. Ansari, K.R.; Quraishi, M.A. Experimental and computational studies of naphthyridine derivatives as corrosion inhibitor for Copper in 15% hydrochloric acid. *Physica E* **2015**, *69*, 322–331.
24. Ansari, K.R.; Quraishi, M.A.; Singh, A.; Ramkumar, S.; Obot, I.B. Corrosion inhibition of Copper in 15% HCl by pyrazolone derivatives: Electrochemical, surface and quantum chemical studies. *RSC Adv.* **2016**, *6*, 24130–24141.
25. Li, X.H.; Deng, S.D.; Fu, H.; Mu, G.N. Inhibition by tween-85 of the corrosion of cold rolled copper in 1.0 M hydrochloric acid solution. *J. Appl. Electrochem.* **2009**, *39*, 1125–1135
26. Singh, A.; Ansari, K.R.; Quraishi, M.A.; Lgaz, H.; Lin, Y. Synthesis and investigation of pyran derivatives as acidizing corrosion inhibitors for Copper in hydrochloric acid: Theoretical and experimental approaches. *J. Alloys Compd.* **2018**, *762*, 347–362.
27. Ansari, K.R.; Quraishi, M.A.; Singh, A. Schiff's base of pyridyl substituted triazoles as new and effective corrosion inhibitors for mild copper in hydrochloric acid solution. *Corros. Sci.* **2014**, *79*, 5–15.
28. Haque, J.; Ansari, K.R.; Srivastava, V.; Quraishi, M.A.; Obot, I.B. Pyrimidine derivatives as novel acidizing corrosion inhibitors for Copper useful for petroleum industry: A combined experimental and theoretical approach. *J. Ind. Eng. Chem.* **2017**, *49*, 176–188.
29. Singh, A.; Ebenso, E.E.; Quraishi, M.A.; Lin, Y. 5, 10, 15, 20-Tetra (4-pyridyl)-21H, 23H-porphine as an effective corrosion inhibitor for Copper in 3.5% NaCl solution. *Int. J. Electrochem. Sci.* **2014**, *9*, 7495–7505.
30. Ansari, K.R.; Quraishi, M.A.; Singh, A. Isatin derivatives as a non-toxic corrosion inhibitor for mild copper in 20% H_2SO_4. *Corros. Sci.* **2015**, *95*, 62–70.
31. Singh, A.; Ansari, K.R.; Kumar, A.; Liu, W.; Songsong, C.; Lin, Y. Electrochemical, surface and quantum chemical studies of novel imidazole derivatives as corrosion inhibitors for J55 copper in sweet corrosive environment. *J. Alloys Compd.* **2017**, *712*, 121–133.
32. Singh, A.; Ansari, K.R.; Xu, X.; Sun, Z.; Kumar, A.; Lin, Y. An impending inhibitor useful for the oil and gas production industry: Weight loss, electrochemical, surface and quantum chemical calculation. *Sci. Rep.* **2017**, *7*, 14904–14921.
33. Singh, A.; lin, Y.; Obot, I.B.; Ebenso, E.E. Macrocyclic inhibitor for corrosion of N80 steel in 3.5% NaCl solution saturated with CO_2. *J. Mol. Liq.* **2016**, *219*, 865–874.
34. Singh, A.; Ansari, K.R.; Chauhan, D.S.; Quraishi, M.A.; Lgaz, H.; Chung, I.M. Comprehensive investigation of steel corrosion inhibition at macro/micro level by ecofriendly green corrosion inhibitor in 15% HCl medium. *J. Colloid Interface Sci.* **2020**, *560*, 225–236.